

# Key Factors Controlling Fibril Formation of Proteins

T.T.M. THU<sup>a,b</sup>, H.N.T. PHUNG<sup>c</sup>,  
N.T. CO<sup>d</sup>, A. KLOCZKOWSKI<sup>e,f</sup> AND M.S. LI<sup>g,\*</sup>

<sup>a</sup>Faculty of Materials Science and Technology, University of Science — VNU HCM, 227 Nguyen Van Cu Street, District 5, Ho Chi Minh City, 700000 Vietnam

<sup>b</sup>Vietnam National University, Area 6, Linh Trung Ward, Thu Duc District, Ho Chi Minh City, 700000 Vietnam

<sup>c</sup>Faculty of Natural Sciences and Technology, Tay Nguyen University, 567 Le Duan street, Buon Me Thuot, Vietnam

<sup>d</sup>Faculty of Chemistry, University of Gdańsk, Fahrenheit Union of Universities, Wita Stwosza 63, 80-308 Gdańsk, Poland

<sup>e</sup>The Steve and Cindy Rasmussen Institute for Genomic Medicine, Nationwide Children's Hospital, 575 Children's Crossroad, Columbus, Ohio 43215, USA

<sup>f</sup>Department of Pediatrics, The Ohio State University College of Medicine, Columbus, Ohio 43215, USA

<sup>g</sup>Institute of Physics, Polish Academy of Sciences, al. Lotników 32/46, PL-02668, Warsaw, Poland

Doi: [10.12693/APhysPolA.145.S21](https://doi.org/10.12693/APhysPolA.145.S21)

\*e-mail: [masli@ifpan.edu.pl](mailto:masli@ifpan.edu.pl)

Fibril formation resulting from protein aggregation is a hallmark of a large group of neurodegenerative human diseases, including Alzheimer's disease, type 2 diabetes, amyotrophic lateral sclerosis, and Parkinson's disease, among many others. Key factors governing protein fibril formation have been identified over the past decades to elucidate various facets of misfolding and aggregation. However, surprisingly little is known about how and why fibril structure is achieved, and it remains a fundamental problem in molecular biology. In this review, we discuss the relationship between fibril formation kinetics and various characteristics, including sequence, mutations, monomer secondary structure, mechanical stability of the fibril state, aromaticity, hydrophobicity, charge, and population of fibril-prone conformations in the monomeric state.

topics: protein fibril formation, aggregation rate, neurodegenerative diseases, amyloid beta peptides

## 1. Introduction

The protein folding takes place in an environment crowded with other biological macromolecules. As a result, proteins are exposed to intermolecular interactions that may lead to aggregation [1]. There are about 50 human diseases characterized by aggregation of proteins [2, 3]. A large number of diseases that can be attributed to amyloidosis are due to the fact that aggregation of pathogenic proteins occurs both in the extracellular space and in the cytoplasm and nucleus. The list of diseases associated with protein aggregation continues to grow. Recently, preeclampsia, a pregnancy-specific disorder, was shown to share pathophysiological features with recognized protein aggregation disorders [4, 5]. Although proteins may vary in sequence, their disease-associated aggregates share a common fibrillar structure known as amyloid fibrils, which have a typical diameter of 7–10 nm and an X-ray diffraction pattern of about 5 Å on the meridian.

Those diseases have common pathogenic pathways, in which protein self-assembly results in irreversible loss of normal structure and function along with the gain of aberrant and debilitating functions.

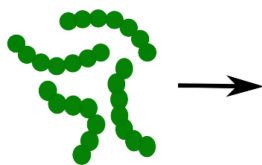
A large body of evidence suggests that amyloid fibrils and associated oligomeric intermediates are related to several neurodegenerative diseases, including Alzheimer's, Parkinson's, Huntington's, prion diseases, type II diabetes, and amyotrophic lateral sclerosis, among others [2, 6]. The most extensively studied case is Alzheimer's disease, which is thought to be associated with abnormal aggregation of so-called beta-amyloid ( $A\beta$ ) peptides.  $A\beta$  peptides, cleaved from the amyloid precursor protein [7], mainly adopt two forms:  $A\beta_{40}$  and  $A\beta_{42}$  peptides, containing 40 and 42 amino acids, respectively. For illustration, in this review we will focus on the aggregation of  $A\beta$  peptides. However, the key factors governing the kinetics of fibril formation should be applied to any protein because they are based on general principles. For example,

## Intrinsic factors

Impact of mutations on aggregation and toxicity of  $A\beta$

### External Factors

Temperature  
Protein concentration  
Pressure  
pH  
Salts  
Ionic strength  
Crowding and confinement  
Foreign surfaces



### Internal Factors

Sequence mutations  
Net charge  
Aromaticity and Hydrophobicity  
Population of fibril-prone state of monomer  
Kinetic stability and mechanical stability of fibril state  
Beta content of monomer

Fig. 1. Internal (group 1) and external (group 2) factors controlling protein aggregation process.

hydrophobicity, which is one such factor, is clearly universal since the stronger the hydrophobic interactions, the faster protein folding and self-assembly occurs.

Although many theoretical and experimental studies have been carried out in recent decades, our understanding of the protein aggregation process remains incomplete. It is not clear why all amyloid fibrils have the common structural feature that is a cross- $\beta$  structure stabilized by backbone hydrogen bonds oriented parallel to the fibril axis. An important question then arises: What factors play a decisive role in the formation of amyloid fibrils? Many review articles have been devoted to this issue [6, 8–13], but none of them fully reflects the overall picture. The purpose of this review is primarily to present the results achieved over the years by our group, as well as the latest achievements of other groups. There are many factors that influence the aggregation process, and they can be divided into two main groups: (i) internal factors related to the intrinsic characteristics of proteins and (ii) external/environmental factors (Fig. 1). The first group refers to the properties of a polypeptide chain, including sequence, ability to resist mechanical forces (mechanical stability), aromaticity, charge, hydrophobicity, and population of the so-called fibril-prone conformation ( $N^*$ ) in a monomeric state [14]. The second group involves external conditions that cause aggregation, such as temperature, pH, salt concentration, and crowding. Here, we focus on the first group of factors, namely the role of mutations, mechanical stability, secondary structures, population of fibril-prone conformations, etc.

## 2. Intrinsic factors

### 2.1. Impact of mutations on aggregation and toxicity of $A\beta$

Alzheimer's disease (AD) is a multifactorial disease with 70% genetic and 30% environmental causes. Among genetic factors are genes associated

with a family history of the disease: familial AD (FAD) and sporadic AD (SAD). Amyloid precursor protein (APP), presenilin 1 (PSEN1), and presenilin 2 (PSEN2) genes are responsible for the occurrence of FAD, while the apolipoprotein E (APOE) gene is responsible for SAD.

We focus on mutations of  $A\beta$  peptides, which are related to FAD because these peptides are cleaved from APP by  $\beta$ - and  $\gamma$ -secretases. Mutations can change the morphology of aggregates and toxicity (Table I [15–45]), and their study is, therefore, important for understanding the molecular mechanism of AD.

Experimental [30, 46–49] and theoretical [50–57] studies revealed that mutations in the turn region such as Flemish (A21G), Dutch (E22Q), Italian (E22K), Arctic (E22G), Iowa (D23N), and Osaka (E22 $\Delta$ , remove glutamic acid) mutants can change aggregation properties. While most of them enhance the toxicity and self-assembly of  $A\beta$ , the Flemish mutant reduces not only the aggregation rate but also toxicity of  $A\beta_{40}$  and  $A\beta_{42}$  [30, 31, 58].  $A\beta_{40}$ (A21G) behaves like the wild-type (WT), but with a slower expansion phase [58]. In line with the conclusion of Betts et al. [58], Murakami et al. [31] observed that the aggregative potency of the Flemish mutant was lowest among the mutants at the 21–23 region, and the thioflavin (ThT) dye fluorescence of this peptide was weaker than WT. In contrast to A21G,  $A\beta_{40}$ (E22G) is more neurotoxic and aggregates faster than the wild-type during both the lag phase and saturation phase. The Arctic mutation also changes the formation of  $A\beta_{40}$  wild-type ( $A\beta_{40}$ -WT) from network-like to annular protofibrils [31, 59]. In  $A\beta_{42}$ , the E22G mutation aggregates slightly slower than WT but increases protofibril formation [31, 32, 59]. In addition, Lo et al. [33] have shown that Arctic (E22G) mutation increases the aggregation rate of  $A\beta$  in micelle solution by decreasing helical structure in the 15–25 segment. Liang et al. [34] studied the three-point mutation of  $A\beta_{40}$  (L17A/F19A/E22G) and found that  $A\beta_{40}$ (E22G) can reduce the toxicity when combined with L17A and F19A by reducing the  $\beta$ -content and by enhancing the  $\alpha$ -helix structure.

Mutations of A $\beta$  peptides and their effect on aggregation rate, toxicity, and aggregate morphology. TABLE I

Mutation	Reference	Aggregation rate	Toxicity	Morphology
A $\beta$ <sub>40</sub> (D1Y)	Maji et al. [15]	reduce	reduce	oligomer long, unbranched fibrils with smooth margin
A $\beta$ <sub>42</sub> (D1Y)	Maji et al. [15]	reduce	reduce	
A $\beta$ <sub>40</sub> (D1E-A2V)	Qahwash et al. [16]	reduce	increase (slightly)	
A $\beta$ <sub>42</sub> (A2F)	Luheshi et al. [17]	increase	increase	straight, unbranched, s 8-nm-diameter fibril
A $\beta$ (pE3-42)	Jawhar et al. [18]	increase	increase	
A $\beta$ <sub>40</sub> (A2V)	Di Fede et al. [19]	increase	increase	
A $\beta$ <sub>42</sub> (A2V)	Di Fede et al. [19], Messa et al [20]	increase	increase	annular oligomer
A $\beta$ <sub>40</sub> (A2T)	Jonsson et al. [21], De Strooper et al. [22]	reduce	reduce	mature fibril oligomer
A $\beta$ <sub>42</sub> (A2T)	Jonsson et al. [21], De Strooper et al. [22]	reduce	reduce	
A $\beta$ <sub>40</sub> (H6R)	Janssen et al. [23], Hori et al. [24]	increase	increase	
A $\beta$ <sub>42</sub> (H6R)	Janssen et al. [23], Hori et al. [24]	increase	increase	mature fibril oligomer
A $\beta$ <sub>40</sub> (D7H)	Hori et al. [24]	increase	increase	
A $\beta$ <sub>42</sub> (D7H)	Hori et al. [24]	increase	increase	
A $\beta$ <sub>40</sub> (D7N)	Hori et al. [24], Wakutani et al. [25], Ono et al. [26]	increase	increase	mature fibril oligomer
A $\beta$ <sub>42</sub> (D7N)	Hori et al. [24], Wakutani et al. [25], Ono et al. [26]	increase	increase	
A $\beta$ <sub>42</sub> (E11K)	Zhou et al. [27]	increase	increase	
A $\beta$ <sub>42</sub> (K16N)	Kaden et al. [28]	increase	reduce	random globular structures
A $\beta$ <sub>40</sub> (K16N)	Kaden et al. [28]	increase	increase	
A $\beta$ <sub>40</sub> (K16A)	Kaden et al. [28], Sinha et al. [29]	reduce	reduce	
A $\beta$ <sub>42</sub> (K16A)	Kaden et al. [28], Sinha et al. [29]	reduce	reduce	Long unbranched fibrils
A $\beta$ <sub>40</sub> (K28A)	Sinha et al. [29]	reduce	reduce	
A $\beta$ <sub>42</sub> (K28A)	Sinha et al. [29]	reduce	reduce	
A $\beta$ <sub>40</sub> (A21G)	Hendricks et al. [30], Murakami et al. [31]	reduce	reduce	ribbon-like structure
A $\beta$ <sub>42</sub> (A21G)	Hendricks et al. [30], Murakami et al. [31]	reduce	reduce	
A $\beta$ <sub>40</sub> (E22Q)	Murakami et al. [31]	increase	increase	
A $\beta$ <sub>42</sub> (E22Q)	Murakami et al. [31]	increase	increase	annular protofibril
A $\beta$ <sub>40</sub> (E22G)	Murakami et al. [31], Nilsberth et al. [32], Lo et al. [33]	increase	increase	
A $\beta$ <sub>42</sub> (E22G)	Murakami et al. [31], Nilsberth et al. [32], Lo et al. [33]	increase	increase	
A $\beta$ <sub>40</sub> (E22G-L17A-F19A)	Liang et al. [34]	reduce	reduce	annular protofibril
A $\beta$ <sub>40</sub> (E22 $\Delta$ )	Ovchinnikova et al. [35], Berhanu et al. [36]	increase	increase	
A $\beta$ <sub>42</sub> (E22 $\Delta$ )	Ovchinnikova et al. [35], Berhanu et al. [36]	increase	increase	
A $\beta$ <sub>40</sub> (E22K)	Murakami et al. [31]	increase	increase	annular protofibril
A $\beta$ <sub>42</sub> (E22K)	Murakami et al. [31]	increase	increase	
A $\beta$ <sub>40</sub> (D23N)	Murakami et al. [31], Qiang et al. [37]	NA	increase	

TABLE I cont.

Mutation	Reference	Aggregation rate	Toxicity	Morphology
A $\beta$ <sub>42</sub> (D23N)	Murakami et al. [31]	reduce	increase	
A $\beta$ <sub>42</sub> (G25L)	Fonte et al. [38], Hung et al. [39]	NA	reduce	
A $\beta$ <sub>42</sub> (G29L)	Fonte et al. [38], Hung et al. [39]	NA	reduce	
A $\beta$ <sub>42</sub> (G33L)	Fonte et al. [38], Hung et al. [39], Decock et al. [40]	increase	reduce	oligomer
A $\beta$ <sub>42</sub> (G37L)	Fonte et al. [38], Hung et al. [39]	NA	reduce	
A $\beta$ (G33L-G38L)	Decock et al. [40]	increase oligomer	NA	oligomer
A $\beta$ <sub>42</sub> (G33A)	Hameier et al. [41]	increase	reduce	
A $\beta$ <sub>42</sub> (G33I)	Hameier et al. [41]	increase	reduce	
A $\beta$ <sub>40</sub> (A30W)	Estrada-Rodríguez et al. [42]	NA	reduce	
A $\beta$ <sub>42</sub> (A30W)	Estrada-Rodríguez et al. [42]	NA	reduce	
A $\beta$ <sub>40</sub> (M35C)	Estrada-Rodríguez et al. [42]	NA	reduce	
A $\beta$ <sub>42</sub> (M35C)	Estrada-Rodríguez et al. [42]	NA	reduce	
A $\beta$ <sub>42</sub> (G37V)	Thu et al. [43]	NA	reduce	ellipse-like
A $\beta$ <sub>42</sub> (V36P-G37P)	Roychaudhuri et al. [44]	reduce	reduce	
A $\beta$ <sub>40</sub> (G33V-V36P-G38V)	Roychaudhuri et al. [44]	increase	increase	
A $\beta$ <sub>42</sub> (G33V-V36P-G38V)	Roychaudhuri et al. [44]	increase	increase	
I41K, A42R, I41D-A42Q, I41D-A42S, I41H-A42D, I41E-A42L, I41H-A42N, I41T-A42N, I41T-A42Q, I41L-A42N, I41Q-A42Y, I41Q-A42L, I41T-A42M, I41T-A42I, I41K-A42L, I41R-A42R	Kim et al. [45]	reduce	NA	

In experimental work on E22Q mutation, Miravalle et al. [60] have shown that after 24 hours of incubation in ThS dye, only A $\beta$ <sub>40</sub>(E22Q) peptide revealed the presence of short filaments with a ribbon-like structure, whereas WT and E22K peptides did not show any presence of the fibrous state. In addition, E22Q has the highest amount of  $\beta$ -structures with the contribution of  $\beta$ -sheets and  $\beta$ -turns. Murakami et al. [31] also revealed that A $\beta$ <sub>42</sub>(E22Q) has the strongest aggregation in the 21–23 region in comparison to WT, Italian, Arctic, and Iowa mutants. Thus, the Dutch (E22Q) mutation was considered the most toxic in the 21–23 region [31, 60]. Similarly to E22Q, Italian (E22K) mutant aggregates faster than WT and has more toxicity for both A $\beta$ <sub>40</sub> and A $\beta$ <sub>42</sub> [31, 60]. These results support the clinical evidence that patients with Dutch and Italian mutations are diagnosed with hereditary cerebral hemorrhage with amyloidosis (HCHWA). Another D23N mutation in the turn region, studied by nuclear magnetic resonance (NMR) spectroscopy by Qiang et al. [37], shows the fibril morphology with the cross  $\beta$  structure. Murakami et al. [31] have shown that A $\beta$ <sub>42</sub>(D23N) (Iowa) mutant has a 2–3-fold more potent cytotoxicity and slightly slower aggregation rate than wild-type A $\beta$ <sub>42</sub>. Deletion of

glutamic acid at residue 22, i.e., E22 $\Delta$  mutation, increases the aggregation rate of A $\beta$ <sub>42</sub> and A $\beta$ <sub>40</sub> peptides, and this mutation is also more toxic than WT [35]. Berhanu et al. [36] have shown that the fibril structure of E22 $\Delta$  is more stable than WT. Glutamic acid (E) is an important amino acid, being acidic polar with a negative charge. When E is substituted by Q or G (neutral amino acids), the primary structure of A $\beta$  changes and the secondary structure also changes, resulting in the enhancement of toxicity. Therefore, decreasing the negative charge at residues 22, 23 of A $\beta$  can increase the aggregation rate and toxicity of this peptide. Electrostatic interactions in this region play an important role in the thermodynamic stability and neurotoxicity of A $\beta$  [61, 62].

Previous studies have shown that the N-terminus region (residues 1–8 of A $\beta$ <sub>40</sub> and 1–16 of A $\beta$ <sub>42</sub>) is disordered in the fibril state [63–66]. NMR spectroscopy studies revealed that the fibril structure of A $\beta$ <sub>42</sub> forms the parallel  $\beta$ -sheet like a “hairpin” [63, 65, 67, 68], and the hydrophilic turn region bends to form the U-shape. Some simulations ignored the N-terminus segment, considering only the 17–42 segment of A $\beta$ <sub>42</sub> or 9–40 of A $\beta$ <sub>40</sub> [69, 70]. However, experimental studies of the whole

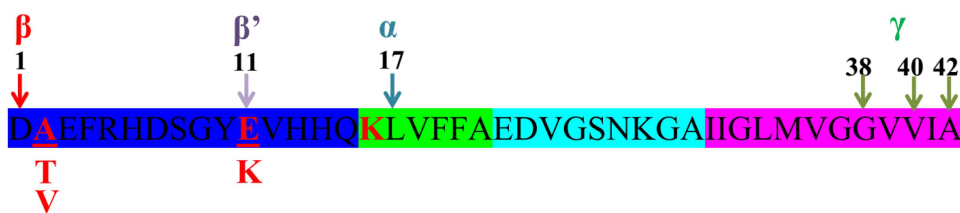


Fig. 2. A2T, A2V, E11K mutations and secretase cleavage sites [27].

structure of A $\beta$ , including the N-terminus region, concluded that residues at the N-terminus region are ordered and play an important role in the whole sequence of A $\beta$  and its toxicity [71–73]. The fibrillar structure of A $\beta$  consists of three  $\beta$ -sheets forming the S-shape [74]. Antibodies bound at the N-terminus interact well with soluble and insoluble A $\beta$  species [75]. Thus, the N-terminal region plays an important role in the A $\beta$  assembly, suggesting that the binding of small molecules in this region may inhibit the A $\beta$ -induced toxicity [76].

The H6R (English) [23, 24], D7H (Taiwanese) [77], and D7N (Tottori) [24–26] mutations were found to stabilize the secondary structure of A $\beta$ , which enhances the aggregation rate [24]. Besides, A $\beta_{40}$ (D7H) has a propensity to form mature fibrils, while A $\beta_{42}$ (D7H) prefers to form oligomers [77]. Experimental studies revealed that the D1Y mutation of A $\beta_{40}$ /A $\beta_{42}$  slows the assembly process [15], while the A2F mutation increases its toxicity [17]. The two-point mutation D1E-A2V influences the fibril morphology of A $\beta_{40}$  [16]. While A $\beta_{40}$  WT forms long fibrillar aggregates, A $\beta_{40}$ (D1E-A2V) develops only protofibrillar morphologies. Cellular toxicity assays indicated that A $\beta_{40}$ (D1E-A2V) was slightly more toxic than A $\beta_{40}$  WT to human neuroblastoma SHEP cells and rat primary cortical and hippocampal neurons. Deletion of the two first residues of A $\beta_{42}$  and the substitution of glutamic acid at the 3<sup>rd</sup> position by pyroglutamic acid, i.e., A $\beta$ (pE3-42), is considered a key factor in the pathology of AD because of the high aggregation propensity of the mutant, its abundance in AD brain, and cellular toxicity [18].

The FAD mutation A $\beta_{40}$ (A2V) causes an early onset of AD [20]. It was revealed that A2V levels up the aggregation kinetics of A $\beta_{40}$ , but the mixture of A $\beta_{40}$  wild-type and A $\beta_{40}$ (A2V) reduces the toxicity of this mutation [19]. For the A $\beta_{42}$  peptide, the A2V mutation has a different fibril morphology and increases the aggregation rate. The fibril of A $\beta_{42}$ (A2V) has the prevalent content of annular structures with higher hydrophobicity and toxicity [20].

In contrast to A2V, the A2T mutation has a strong protective effect, preventing cognitive decline in the elderly without AD [21, 22]. The A2T mutation is located at the second residue in the A $\beta$  peptide, corresponding to residue 673 in APP and nearby  $\beta$ -secretase (residue 672 in APP, see Fig. 2).

Zhou et al. [27] studied E682K mutation (site of  $\beta'$  enzyme in Fig. 2) on APP, corresponding to E11K on A $\beta_{42}$ . They showed that E11K enhances the formation of A $\beta$  from APP by  $\beta$ ,  $\beta'$ , and  $\gamma$  enzymes [27] (Fig. 2). Therefore, individuals having this mutation can get AD at age 49–53, i.e., earlier than others [27]. Kaden et al. [28] reported that the K16N mutation (site of enzyme  $\alpha$  in Fig. 2) enhances the toxicity of A $\beta$  when mixing K16N and WT. The aggregate of this mutation has an oligomeric structure of various sizes. Replacing K with A at residue 16, the K16A mutation reduces the toxicity of A $\beta$  by changing the morphology of aggregates and increasing the content of the  $\alpha$ -structure [28, 29]. Sinha et al. [29] studied the K28A mutation, showing that the substitution of lysine by alanine inhibits A $\beta$  toxicity. In addition, the K28A mutation reduces the process of conversion in the secondary structure and enhances the random coil structure. These observations support the hypothesis that Lys28 stabilizes the nucleation phase in the fibrillization process proposed by Lazo et al. [78].

The C-terminus region (residues 31–40/31–42) of A $\beta$  is stable and plays a key role in aggregation and binding with other ligands [79, 80]. Thus, mutations in this area are of great interest. The glycine zipper motif at the C-terminus, including glycine at residues 25, 29, 33, 37, can influence the transformation of a random helix or  $\alpha$ -helical structure into a  $\beta$ -sheet and, therefore, fibril formation. Destabilizing this structure by mutations is an effective way to study its role [38–41]. Mutants G25L, G29L, G33L, and G37L, where glycine was replaced by leucine, were shown to be less toxic than A $\beta_{42}$  WT in mouse primary cortical neurons [39]. Research by Fonte et al. [38] supports this idea; in particular, G37L reduces the toxicity of A $\beta$  in all models tested. The G33L mutation enhances the oligomer structure of A $\beta$  [41], but when mixed with G38L, this effect becomes weaker [40]. Thu et al. [43] replaced glycine with valine at residue 37 and found that the G37V mutation did not change the rate of aggregation but reduced the toxicity and changed the fibril morphology from network to ellipse-like shape.

*In vitro* and *in vivo* experiments showed that A $\beta_{42}$  oligomers with the replacement of glycine 33 by isoleucine and alanine are much less toxic than A $\beta_{42}$  WT [41]. In addition, mutations G33A and G33I promoted aggregation by increasing the

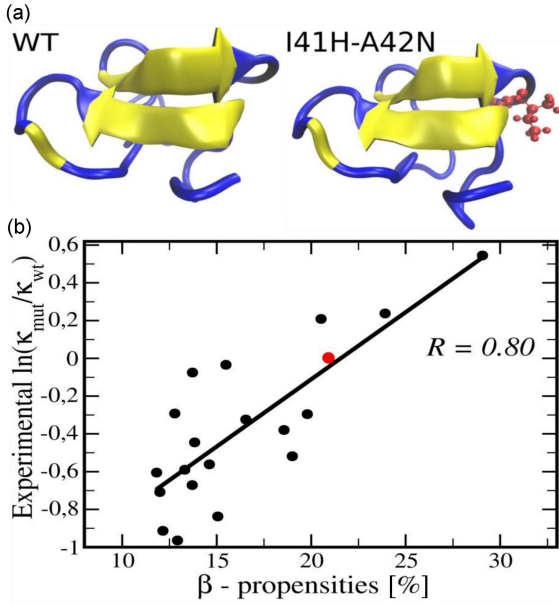


Fig. 3. Initial structure for MD simulation of  $A\beta_{42}$ -WT and I41H-A42N mutation; mutated residues are in red (panel a). Dependence of the logarithm of the relative aggregation rate on  $\beta$ -content; the red circle refers to WT. Linear fit is  $y = -1.534 + 0.071x$  ( $R = 0.80$ ) (panel b) [83]. References to experimental data shown in this figure can be found in [83].

population of large oligomers (16- to 20-mers) at the expense of small oligomers (2- to 4-mers). Recently, Rodríguez et al. [42] have studied one-point mutations K28A, A30W, and M35C on the 25–35 segment of  $A\beta$ . They have found that fibril formation was more dependent on the primary sequence of peptides than on their length. Mutations A30W and M35C reduced toxicity by the reducing production of reactive oxygen species (ROS) but did not affect the aggregation rate. Thus, the primary sequence is most important for the cytotoxicity of  $A\beta$ .

In another study, Roychaudhuri et al. [44] found that the  $\beta$ -hairpin motif with a  $\beta$ -turn at residues Val36-Gly37 is highly populated in  $A\beta_{31-42}$  but does not exist in  $A\beta_{31-40}$ . In addition, the three-point mutation G33V-V36P-G38V (VPV) levels up the  $\beta$ -turn and  $\beta$ -hairpin content at the C-terminus, increases cytotoxicity, and alters the aggregate morphology. The VPV mutation makes  $A\beta_{40}$  oligomerization as fast as  $A\beta_{42}$ , while  $A\beta_{42}$  becomes “super  $A\beta_{42}$ ”. In contrast to VPV, the V36P-G37P two-point mutation of  $A\beta_{42}$  produces  $A\beta_{40}$ -like oligomers instead of forming hexamers and dodecamers. This study showed that the V36P-G37P mutation leads to the abolishment of  $\beta$ -turn formation at residues 36–37 and reduces the  $\beta$ -content and toxicity of  $A\beta_{42}$  [79]. Linh et al. [81] performed all-atom molecular dynamics (MD) simulations of the full-length  $A\beta_{40}$  and  $A\beta_{42}$  and obtained results

different from those of Roychaudhuri et al. [44], indicating that the VPV mutation promotes the  $\beta$ -turn structure at residues 36–37 but is insufficient to make  $A\beta_{40}$ (VPV) oligomerization to become like  $A\beta_{42}$  WT [81]. Besides, the  $\beta$ -hairpin motif at residues 36–37 present in  $A\beta_{42}$  WT does not appear in  $A\beta_{40}$ (VPV).

Kim et al. [45] synthesized mutants by replacing I41 and A42 with less hydrophobic amino acids. They showed that substitution of these residues with negatively charged hydrophilic amino acids (I41D-A42Q, I41D-A42S, I41H-A42D, I41E-A42L), neutral hydrophilic amino acids (HN, TN, TQ, LN, QY, QL, TM, TI), or positively charged residues (I41K, KL, RR, A42R), slows aggregation. Thus, the last two residues, namely I41 and A42, play an important role in the aggregation process and toxicity of  $A\beta_{42}$ . Table I shows mutations in  $A\beta$  peptides and their impact on various properties.

## 2.2. Beta-content in monomeric state

The influence of secondary structure on the aggregation rate of protein was studied indirectly by Chiti et al. [82] by finding the effect of the free energy change in conversion from the  $\alpha$ -helix to  $\beta$ -sheet conformation ( $\Delta\Delta G$ ). The equation representing the correlation between the combination of  $\Delta\Delta G$ , the change in hydrophobicity ( $\Delta\text{Hydr}$ ), and the change in charge ( $\Delta\text{Charge}$ ) with the aggregation rates for the mutant  $\kappa_{\text{mut}}$  and the wild-type  $\kappa_{\text{wt}}$  is [82]

$$\ln\left(\frac{\kappa_{\text{mut}}}{\kappa_{\text{wt}}}\right) = A\Delta\Delta G + B\Delta\text{Hydr} + C\Delta\text{Charge}. \quad (1)$$

By choosing the appropriate fit parameters  $A$ ,  $B$ , and  $C$ , a high correlation between these quantities was found. Recently, Thu et al. [83] have calculated the  $\beta$ -content of 19 mutations of  $A\beta_{42}$  using replica exchange molecular dynamics simulation in implicit water. They showed that the experimentally measured aggregation rate  $\kappa$  depends on the calculated  $\beta$ -content in monomeric state  $\kappa = \kappa_0 \exp(c\beta)$ ,  $c = 0.071$  with the correlation level  $R = 0.80$  (Fig. 3b). Thus, the higher the  $\beta$ -propensity, the faster formation of fibrils. It would be interesting to test this conclusion on other systems.

## 2.3. Population of fibril-prone state in monomeric state

It is known that in the monomeric native state, the protein is compact, and in the fibrillar state, it forms an expanded  $\beta$ -structure, which is called the fibril-prone state  $\mathbf{N}^*$ . Consequently,  $\mathbf{N}^*$  is an excited state in the energy spectrum of the monomer [84]. In lattice models, for a chain with a sufficiently small number of beads, it is possible

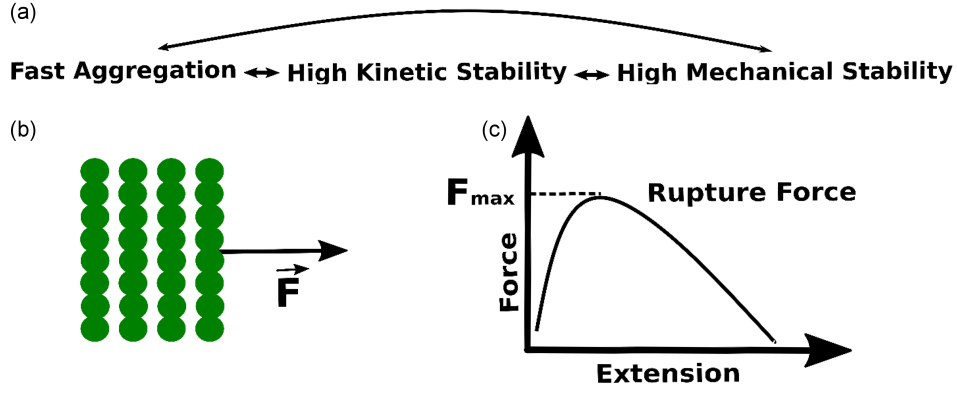


Fig. 4. (a) Relationship between aggregation rate, kinetic stability, and mechanical stability of the fibril state. (b) Pulling a chain from the fibrillar structure to probe its mechanical stability. (c) Force-extension profile with the rupture force defined as  $F_{\max}$ .

to perform an exact search of all possible conformations and find the full energy spectrum. The fibril-prone state population is then defined as

$$P_{N^*} = \frac{1}{Z} \exp\left(-\frac{E_{N^*}}{k_B T}\right), \quad (2)$$

$$Z = \sum_{i=1}^N e^{-E_i/(k_B T)}, \quad (3)$$

where  $Z$  is the partition function,  $E_{N^*}$  is the energy of the  $N^*$  state,  $E_i$  is the energy of the  $i$ -th state, and  $N$  is the total number of states. However, in most cases (continuum models or lattice models with long chains), the exact energy spectrum cannot be found, and (2) cannot be used to calculate  $P_{N^*}$ . In this situation the population of fibril-prone state is approximately estimated using simulations. Namely,  $P_{N^*}$  is defined as the time of the appearance of the  $N^*$  state during the entire simulation divided by the total simulation time.

Li et al. [14] proposed that the higher the population, the faster the rate of fibril formation. The rationale for this hypothesis is that the  $N^*$  state can serve as a template for fibril formation, and its high population will promote this process. Using the toy lattice model [84], it was shown that the fibril formation rate decreases exponentially with increasing  $P_{N^*}$ ,

$$\kappa \sim \exp(-cP_{N^*}), \quad (4)$$

where the constant  $c$  depends on the studied models and systems. The validity of the  $N^*$ -theory (see (4)) has been confirmed for all-atom [85] and off-lattice coarse-grained models [86]. Recently, using the coarse-grained self-organized polymer-intrinsically disordered protein (SOP-IDP) model [87] and MD simulations, Chakraborty et al. [88] have shown that  $P_{N^*}$  of  $A\beta_{42}$  is larger than that of  $A\beta_{40}$ , which indicates that, in agreement with experiment [89], the former aggregates faster than the latter due to the two terminal hydrophobic residues. It was shown that the population of the  $N^*$  state depends on the morphology of fibrils, implying that the shape

of the aggregate depends on the time of its formation. In other words, the  $N^*$ -theory ascertains that fibrillar polymorphism is time-dependent or under kinetic control [90]. Assuming that the fibril formation obeys Ostwald's rule, which states that the least stable polymorph would form first, followed by a subsequent transition to a more stable form, Chakraborty et al. [88] predicted that the S-bend  $A\beta_{42}$  fibril is more stable than the U-bend form, as the latter forms faster.

#### 2.4. Mechanical stability of the fibril state

Kouza and co-workers [91] proposed a new definition of the kinetic stability ( $G_{fib}$ ) of the fibrillar state based on the probability ( $P_{fib}$ ) of reaching the fibrillar configuration, i.e.,

$$G_{fib} = -k_B T \ln(P_{fib}), \quad (5)$$

$$\tau_{fib} = \exp(aG_{fib}). \quad (6)$$

Their computational study also indicated that the fibril formation time ( $\tau_{fib}$ ) showed no clear correlation with the fibril state energy ( $E_{fib}$ ) or the free energy of the system. Instead,  $\tau_{fib}$  displayed an exponential dependence on  $G_{fib}$  (see (6)). This relationship between  $G_{fib}$  and  $\tau_{fib}$  can be interpreted as evidence that the kinetic stability of the fibrillar state correlates with the rate of fibril formation. Moreover, this relationship can be qualitatively understood using the framework shown in Fig. 4a. On the one hand, the higher the mechanical stability, the higher the kinetic stability, determined by (5). On the other hand, the higher the kinetic stability, the faster the aggregation occurs. Consequently, the higher the mechanical stability of the fibrillar state, the faster the fibril formation.

The mechanical stability of the fibril can be accessed using steered molecular dynamics (SMD) simulations [91]. Namely, this mechanical stability can be characterized by the rupture force or the maximum force in the force-extension/time profile

obtained by pulling a single chain from the fibril structure (Fig. 4b and c). Using all-atom models to calculate mechanical stability and fibril formation time for short peptides such as KLVFF and FVFLM, the relationship between these two quantities was confirmed [91].  $A\beta_{42}$  has been experimentally shown to form fibril faster than  $A\beta_{40}$  [71, 89], which is consistent with SMD simulations that the former is mechanically more stable than the latter [91]. By performing all-atom SMD simulations for 20  $A\beta_{42}$  mutants whose aggregation rates are known from experiments, Thu and Li [92] obtained clear evidence that the aggregation rate correlates with the mechanical stability of the fibrillar structure. Since calculating fibril formation times for relatively large proteins using all-atom models is computationally prohibitive, this relationship is very useful as it allows us to estimate  $\tau_{fib}$  from the rupture force, which can be easily obtained from SMD simulations.

### 3. External factors

The process of protein folding, which involves the transformation of proteins into their three-dimensional functional conformations or native states, serves as a core principle in structure biology. However, proteins are also prone to adopting energetically preferential aggregated configurations, a phenomenon known as protein misfolding or aggregation. Numerous variables, including the inherent characteristics of the proteins, the environmental physical conditions, or the overcapacity of the regulatory systems, potentially influence this process. Figure 1 illustrates the standard external factors that contribute to the protein aggregation process.

#### 3.1. Temperature

Thermal variations have a significant impact on the process of associating monomers into higher-ordered structures [9, 93, 94]. A significant enhancement in the aggregation rate of  $\beta$ -lactoglobulin was observed as the temperature shifted from 30 to 50°C [95]. The temperature range of 29–45°C and 4–40°C was reported to elicit an acceleration in the nucleation and elongation phases of self-assembly for  $A\beta$  peptides [96, 97]. Elevated temperatures can cause the protein to deviate from its native conformation, resulting in partially or fully denatured states in which hydrophobic regions are exposed to the solvent environment. The presence of such hydrophobic cores, as a result of thermal denaturation, increases the likelihood of intermolecular interactions between proteins, leading to the acceleration of the aggregation process [98, 99]. It is noteworthy that a specific subset of proteins exhibits a phenomenon known as cold-induced denaturation, where the stability of the native structure is lost at

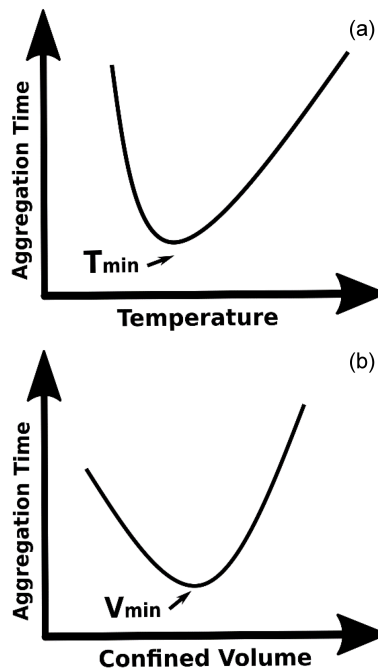


Fig. 5. U-shape dependence of aggregation time on temperature (a) and confined volume (b). The fastest aggregation occurs at  $T_{min}$  and  $V_{min}$ .

low temperatures, resulting in the acceleration of the condensation process [100, 101]. Self-assembly of ribosomal protein L9 occurs faster at 4°C than at 25°C [101]. The reduction of temperature from 37 to 5°C catalyzed the monoclonal antibody aggregation [102]. The adherence of temperature-dependent rate of aggregation of certain proteins to the traditional Arrhenius law was observed within a narrow temperature range [103–105]. Nevertheless, the Arrhenius law may not govern the behavior of proteins within a wider temperature range [94, 106–109].

The complex effect of temperature on proteins, both direct and indirect, influences the self-assembly process in multiple ways. However, in general, the temporal dependence of aggregation on temperature can be understood as the trade-off between the entropy and energy of the studied system, which is typically characterized by a U-shaped form (Fig. 5a). The minimum aggregation time is attained at the optimal temperature ( $T_{min}$ ) that corresponds to the highest rate of aggregation [110].

#### 3.2. Protein concentration

The concentration of proteins plays a pivotal role in modulating protein aggregation propensity because it significantly influences both the intermolecular distances and the interaction among protein molecules. The critical concentration is defined as the concentration above which protein self-assembly occurs. This concentration depends on the specific type of protein and typically fluctuates within



the micro-molar to nano-molar range in biophysical conditions. Polyglutamine (polyQ) [111],  $\beta$ -ovalbumin [112], and  $\alpha$ -synuclein [113] initiate their self-assembly at respective concentrations approximating 3  $\mu$ M, 7  $\mu$ M, and 0.7  $\mu$ M. For  $A\beta_{42}$  and  $A\beta_{40}$  peptides, their assembly thresholds are in the  $\mu$ M range [114, 115] and could potentially reach nM levels [116]. Furthermore, an increase in monomer concentration results in a decrease in both the lag time as well as the overall time required for aggregation owing to the intensification of collision frequencies among the monomers [113]. Nevertheless, high protein concentration can result in the retardation of aggregation [117, 118] due to the trade-off between on-pathway and off-pathway oligomers [119].

In the case of protein self-assembly via the primary nucleation mechanism, the relation between characteristic times  $\tau_F$  (for instance, lag time or half time) and the concentration  $c$  is represented by  $\tau_F \approx c^{-(n_c+1)/2}$  [120], where  $n_c$  is the size of the critical nucleus. It is worth noting that a distinct dependence on concentration has been discerned in the scenario of secondary nucleation [121].

### 3.3. Pressure

High hydrostatic pressure exerts influences on the conformation of proteins, the interactions between proteins, and the formation of polymers or aggregates through volume modifications [122]. Some studies suggested that the volumetric fluctuation arising from the exclusion of water from internal cavities [123, 124], the hydration of hydrophobic surfaces [125], the dissociation, and the rupture of associated ion-pair interactions [126] are the underlying causes of pressure-induced protein unfolding and may have a consequential impact on protein aggregation rates under high-pressure conditions [127–129].

### 3.4. pH

The acidity of a solution (pH) plays a role in the charge density of the protein surface. A highly acidic pH environment causes a concentration of similar charges on the surface of peptides, leading to strong repulsion and hindering the self-assembly of peptide molecules. For instance, the formation of salt bridges between Lys28 and Asp23 is prevented due to the neutralization of residue Lys28 at pH levels greater than 9.5, resulting in the inhibition of the self-assembly of peptides  $A\beta_{42}$  [130]. Generally, the tendency for protein to aggregate increases at pH values near the isoelectric point of the protein [131].

### 3.5. Ionic strength

The kinetics of protein aggregation, as well as the morphological characteristics of aggregated products, are significantly influenced by the ionic

strength of the surrounding medium. Multiple deposition forms of  $\alpha$ -synuclein were noted by Hoyer et al. [132] within NaCl and MgCl<sub>2</sub> solutions. Amyloid fibrillogenesis of  $\beta_2$ -microglobulin was affected by the addition of anions SO<sub>4</sub><sup>2-</sup>, Cl<sup>-</sup>, I<sup>-</sup>, ClO<sub>4</sub><sup>-</sup> to the solution [133]. Other investigations have explored the impacts of ionic strength on the propensity for aggregation in proteins such as  $\beta$ -lactoglobulin [134], islet amyloid polypeptide (IAPP) [135],  $A\beta_{40}$  [136], or  $A\beta_{42}$  [137].

### 3.6. Salts

In solution, the binding of unpaired charged residues or backbones of proteins with the cations and anions generated from salt dissolution can lead to alterations in protein structures and protein dissolution capacity or affect inter-protein interactions, thereby influencing the propensity for protein self-assembly [138–140]. Adding salt ions to the solution of HCA II at temperature 328 K switched HCA II aggregation behavior from a monophasic to a biphasic mechanism [141]. The competitive formation of amyloids versus amorphous aggregates was observed by Adachi et al. [142] as they were studying the effect of varying NaCl concentration on the aggregation rate of  $\beta_2$ -microglobulin — bovine serum albumin kinetics changed from downhill to nucleation-dependent kinetics in the presence of guanidinium hydrochloride (GdmCl) and CaCl<sub>2</sub> in the studied solution [143]. NaCl can increase the rhGCSF aggregation rate [144], yet it can also impede the self-assembly capacity of the recombinant factor VIII SQ [145].

### 3.7. Crowding and confinement

Protein misfolding and aggregation occur in an environment that includes a variety of components called crowders. In biological organisms, crowders, including proteins, sugars, lipid membranes, chaperones, nucleic acids, collagen, and others, can account for up to 40% of living matter [146–148]. *In vitro* settings, crowders can be artificially introduced substances such as nanoparticles [149] or polymers [150]. Crowders can speed up the self-assembly process of proteins, which is primarily explained by their volume exclusion effect, which narrows the spatial region available to proteins and thereby reduces their entropic cost [151–155]. In contrast, in a densely populated environment with sufficiently small particles, the aggregation process may be slowed due to diffusion restrictions imposed on peptides by crowders [149, 156, 157] or the potential deformation of proteins from their aggregation-prone states [158].

Often intertwined in discussions due to their strong correlation, crowding and confinement are distinct yet related concepts in protein aggregation. Crowding refers to the densely populated milieu

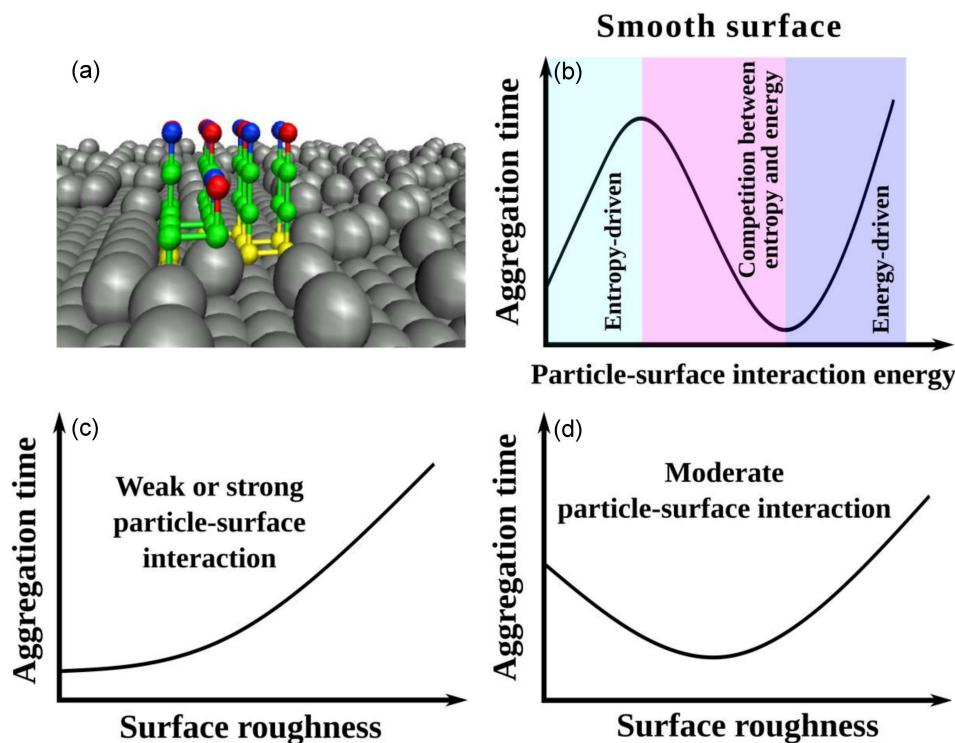


Fig. 6. Deposition of six peptides on the rough surface in the lattice model (a), the effect of varying protein–smooth surface interaction energy on the protein aggregation time (b), the relation between the aggregation time and roughness degree of foreign surfaces under the conditions of small and high (c), and moderate (d) particle–surface interactions. Weak, moderate, and strong particle–surface interactions in (c) and (d) correspond to entropy-driven, entropy–energy competition, and energy-driven regimes in (b).

in which the aggregation occurs, whereas confinement addresses the association of proteins within the fixed or rigid structures, which may include chaperones, ribosome exit tunnels, or cytoskeleton [159]. The interplay between entropy and energy in proteins manifests as a U-shaped curve representing the dependence of protein aggregation rate on confined volume (Fig. 5b). In highly confined spaces, the restriction of the conformational entropy of proteins prevents them from reaching an optimal energy state, hence significantly elongating the aggregation time. Conversely, as the volume of confinement increases, the protein conformational entropy experiences a sharp increase, which in turn leads to a slowdown in the aggregation process [156].

### 3.8. Foreign surfaces

The phenomena of protein aggregation are not limited to solution environments but are also observed under various surface conditions. Although the presence of foreign surfaces can be perceived as crowding agents, their role extends beyond the traditional crowding concept, which primarily captures the global effects of the environment on protein self-assembly. Indeed, the influence of foreign surfaces on protein aggregation has received considerable attention due to their wide range of applications

spanning drug discovery, new materials development, and polymer science [160–162]. Foreign surfaces can potentially expedite the aggregation process; numerous lipid membranes, for instance, have been observed to catalyze fibril growth [163–165]. Other examples include mica and glass surfaces, which have been reported to act as catalysts in the fibrillation of  $\alpha$ -synuclein [166] and  $A\beta_{18-22}$  [167]. Conversely, certain external surfaces may have a suppressive influence on the assembly of amyloid fibrils; in particular, the deposition of IAPP was notably inhibited in a milieu containing surfaces coated with polymeric nanoparticles [149], as well as the self-assembly of  $A\beta_{42}$  into fibril-like structures was slowed down by protein-coated surfaces of graphene oxide [168]. Additionally, the interaction between proteins and surfaces could extend to the modification of fibril morphology [169, 170], sometimes up to the complete alternation of their fibrillar structures [171]. Furthermore, the aggregation propensity of proteins has been demonstrated to be sensitive to changes in surface topography [172] and the degree of surface roughness [173, 174], highlighting the intricate and subtle nature of protein–surface interactions.

Applying a simple lattice model for investigating the aggregation of 8-bead chains on both smooth and rough surfaces (Fig. 6a), Co and Li [174] proposed a general scheme for understanding the

self-assembly in the presence of foreign surfaces. They found that due to the trade-off between entropy and energy, a moderately absorbing smooth surface promoted protein aggregation, while weakly and strongly absorbing surfaces hindered the process (Fig. 6b). For rough surfaces, both weakly and highly absorbent surfaces tended to increase the duration of the aggregation process (Fig. 6c). However, moderately absorbent surfaces showed a dual effect, i.e., at higher roughness levels, these surfaces inhibited protein deposition, whereas at lower roughness levels, they catalyzed the aggregation process (Fig. 6d).

### 3.9. Other external factors

Here we list other external factors that are not discussed in this review: oxidative stress [175, 176], organic solvent [177], ligands [178], freezing [179], thawing [180], metal ions [181, 182], UV illumination [183], drying [184], pumping [185], surfactants [186], biopolymer [187], interface- and mechanical-force-mediated amyloid formation [188].

## 4. Conclusions

In this review, we have focused on new developments related to intrinsic and external factors that can influence protein aggregation. For many decades, protein folding research has been dominated by the assumption that thermodynamics determines protein structure and function. However, recent experimental evidence supports the newly emerging paradigm of non-equilibrium control of protein behavior [189]. Specifically, the speed of synthesis of proteins in the ribosome greatly influences their properties, mRNA sequence evolution, and disease. Consequently, studying the effect of translation kinetics on protein misfolding, aggregation [190], and related diseases will be of great interest in the near future.

The relationship between viruses and amyloids is attracting more attention.  $A\beta$  aggregation, for example, was found to be promoted by the HSV-1 viral corona both *in vitro* and *in vivo* [191]. The SARS-CoV-2 nucleocapsid protein (N protein) accelerates  $\alpha$ S fibrillation through electrostatic interactions, inducing cell death [192]. It has been shown that SARS-CoV-2 proteins can also form aggregates in isolation [193, 194], and similar results have been obtained for other virus species, such as the Hendra and Nipah viruses [195]. Based on the observation that human amyloids can interact with viruses, interfering with their replication, protein aggregation has been proposed as a strategy to discover new antiviral agents [196]. Thus, identification of the underlying factors that control virus-amyloid interactions is an important research direction in life sciences.

Finally, the main topic of this review resonates with the work of Professor Marek Cieplak on protein droplets, amyloid glass phase in systems of disordered homopeptides [197], and liquid-liquid phase separation [198]. The mechanical stability of fibrils discussed here is related to the protein and capsid stability studied by M. Cieplak et al. [199, 200] using simple Go models. His work in this direction had a high impact on the computational community because it showed that many important results could be obtained with simple models that did not require time-consuming simulations. In particular, his contributions influenced the development of some of the ideas presented in this article.

## Author's Contribution

All authors contributed to discussion of topics and writing of the review. T.T.M. Thu and H.N.T. Phung contributed equally.

## Acknowledgments

TTMT was funded by Vietnam National University, Ho Chi Minh City (VNU-HCM), under grant number C2020-18-19.

## References

- [1] C.M. Dobson, *Nature* **426**, 884 (2003).
- [2] F. Chiti, C.M. Dobson, *Ann. Rev. Biochem.* **75**, 333 (2006).
- [3] C.M. Dobson, *Cold Spring Harb. Perspect. Biol.* **9**, a023648 (2017).
- [4] I.A. Buhimschi, U.A. Nayeri, G. Zhao, L.L. Shook, A. Pensalfini, E.F. Funai, I.M. Bernstein, C.G. Glabe, C.S. Buhimschi, *Sci. Trans. Med.* **6**, 245ra292 (2014).
- [5] M. Kouza, A. Banerji, A. Kolinski, I.A. Buhimschi, A. Kloczkowski, *Phys. Chem. Chem. Phys.* **19**, 2990 (2017).
- [6] P.H. Nguyen, A. Ramamoorthy, B.R. Sahoo et al., *Chem. Rev.* **121**, 2545 (2021).
- [7] D.J. Selkoe, *Nat. Cell Biol.* **6**, 1054 (2004).
- [8] M.C. Owen, D. Gnutt, M. Gao, S.K.T.S. Wärmländer, J. Jarvet, A. Gräslund, R. Winter, S. Ebbinghaus, B. Strodel, *Chem. Soc. Rev.* **48**, 3946 (2019).
- [9] R. Rajan, S. Ahmed, N. Sharma, N. Kumar, A. Debas, K. Matsumura, *Mater. Adv.* **2**, 1139 (2021).
- [10] S. Devi, M. Chaturvedi, S. Fatima, S. Priya, *Toxicology* **465**, 153049 (2022).
- [11] T. Sinnige, *Chem. Sci.* **13**, 7080 (2022).

- [12] J. Sheng, N.K. Orlachs, B.M. Gadella, D.V. Kaloyanova, J.B. Helms, *Int. J. Mol. Sci.* **21**, 6530 (2020).
- [13] P. Alam, K. Siddiqi, S.K. Chturvedi, R.H. Khan, *Int. J. Biol. Macromol.* **103**, 208 (2017).
- [14] M.S. Li, N.T. Co, G. Reddy, C.K. Hu, J.E. Straub, D. Thirumalai, *Phys. Rev. Lett.* **105**, 218101 (2010).
- [15] S.K. Maji, R.R.O. Loo, M. Inayathullah, S.M. Spring, S.S. Vollers, M.M. Condrón, G. Bitan, J.A. Loo, D.B. Teplow, *J. Biol. Chem.* **284**, 23580 (2009).
- [16] I. Qahwash, K.L. Weiland, Y. Lu, R.W. Sarver, R.F. Kletzien, R. Yan, *J. Biol. Chem.* **278**, 23187 (2003).
- [17] L.M. Luheshi, G.G. Tartaglia, A.-C. Brorsson, A.P. Pawar, I.E. Watson, F. Chiti, M. Vendruscolo, D.A. Lomas, C.M. Dobson, D.C. Crowther, *PLoS Biol.* **5**, e290 (2007).
- [18] S. Jawhar, O. Wirths, T.A. Bayer, *J. Biol. Chem.* **286**, 38825 (2011).
- [19] G. Di Fede, M. Catania, M. Morbin et al., *Science* **323**, 1473 (2009).
- [20] M. Messa, L. Colombo, E. Del Favero, L. Cantù, T. Stoilova, A. Cagnotto, A. Rossi, M. Morbin, G. Di Fede, F. Tagliavini, *J. Biol. Chem.* **289**, 24143 (2014).
- [21] T. Jonsson, J.K. Atwal, S. Steinberg, J. Snaedal, P.V. Jonsson, S. Bjornsson, H. Stefansson, P. Sulem, D. Gudbjartsson, J. Maloney, *Nature* **488**, 96 (2012).
- [22] B. De Strooper, T. Voet, *Nature* **488**, 38 (2012).
- [23] J. Janssen, J. Beck, T. Campbell, A. Dickinson, N. Fox, R. Harvey, H. Houlden, M. Rossor, J. Collinge, *Neurology* **60**, 235 (2003).
- [24] Y. Hori, T. Hashimoto, Y. Wakutani, K. Urakami, K. Nakashima, M.M. Condrón, S. Tsubuki, T.C. Saido, D.B. Teplow, T. Iwatsubo, *J. Biol. Chem.* **282**, 4916 (2007).
- [25] Y. Wakutani, K. Watanabe, Y. Adachi, K. Wada-Isoe, K. Urakami, H. Ninomiya, T. Saido, T. Hashimoto, T. Iwatsubo, K. Nakashima, *J. Neurol. Neurosurg. Psychiatry* **75**, 1039 (2004).
- [26] K. Ono, M.M. Condrón, D.B. Teplow, *J. Biol. Chem.* **285**, 23186 (2010).
- [27] L. Zhou, N. Brouwers, I. Benilova, A. Vandersteen, M. Mercken, K. Van Laere, P. Van Damme, D. Demedts, F. Van Leuven, K. Sleegers, *EMBO Mol. Med.* **3**, 291 (2011).
- [28] D. Kaden, A. Harmeier, C. Weise, L.M. Munter, V. Althoff, B.R. Rost, P.W. Hildebrand, D. Schmitz, M. Schaefer, R. Lurz, *EMBO Mol. Med.* **4**, 647 (2012).
- [29] S. Sinha, D.H. Lopes, G. Bitan, *ACS Chem. Neurosci.* **3**, 473 (2012).
- [30] L. Hendriks, C.M. Van Duijn, P. Cras, M. Cruts, W. Van Hul, F. Van Harskamp, A. Warren, M.G. McInnis, S.E. Antonarakis, J.-J. Martin, *Nat. Genet.* **1**, 218 (1992).
- [31] K. Murakami, K. Irie, A. Morimoto, H. Ohigashi, M. Shindo, M. Nagao, T. Shimizu, T. Shirasawa, *J. Biol. Chem.* **278**, 46179 (2003).
- [32] C. Nilsberth, A. Westlind-Danielsson, C.B. Eckman et al., *Nat. Neurosci.* **4**, 887 (2001).
- [33] C.J. Lo, C.C. Wang, H.B. Huang, C.F. Chang, M.S. Shiao, Y.C. Chen, T.H. Lin, *Amyloid* **22**, 8 (2015).
- [34] C.T. Liang, H.B. Huang, C.C. Wang, Y.R. Chen, C.F. Chang, M.S. Shiao, Y.C. Chen, T.H. Lin, *PLoS One* **11**, e0154327 (2016).
- [35] O.Y. Ovchinnikova, V.H. Finder, I. Vodopivec, R.M. Nitsch, R. Glockshuber, *J. Mol. Biol.* **408**, 780 (2011).
- [36] W.M. Berhanu, E.J. Alred, U.H. Hansmann, *J. Phys. Chem. B* **119**, 13063 (2015).
- [37] W. Qiang, W.M. Yau, Y. Luo, M.P. Mattson, R. Tycko, *Proc. Natl. Acad. Sci. USA* **109**, 4443 (2012).
- [38] V. Fonte, V. Dostal, C.M. Roberts, P. Gonzales, P. Lacor, J. Magrane, N. Dingwell, E.Y. Fan, M.A. Silverman, G.H. Stein, *Mol. Neurodegener.* **6**, 61 (2011).
- [39] L.W. Hung, G.D. Ciccotosto, E. Giannakis, D.J. Tew, K. Perez, C.L. Masters, R. Cappai, J.D. Wade, K.J. Barnham, *Neurosci. J.* **28**, 11950 (2008).
- [40] M. Decock, S. Stanga, J.-N. Octave, I. Dewachter, S.O. Smith, S.N. Constantinescu, P. Kienlen-Campard, *Front. Aging Neurosci.* **8**, 107 (2016).
- [41] A. Harmeier, C. Wozny, B.R. Rost, L.-M. Munter, H. Hua, O. Georgiev, M. Beyermann, P.W. Hildebrand, C. Weise, W. Schaffner, *Neurosci. J.* **29**, 7582 (2009).
- [42] A.E. Estrada-Rodríguez, D. Valdez-Pérez, J. Ruiz-García, A. Treviño-Garza, A.M. Gómez-Martínez, H.G. Martínez-Rodríguez, A.M. Rivas-Estilla, R. Vidal-tamayo, V. Zomosa-Signoret, *Int. J. Pept. Res. Ther.* **25**, 493 (2019).

- [43] T.T.M. Thu, S.-H. Huang, L.A. Tu, S.-T. Fang, M.S. Li, Y.-C. Chen, *Neurochem. Int.* **129**, 104512 (2019).
- [44] R. Roychaudhuri, M. Yang, A. Deshpande, G.M. Cole, S. Frautschy, A. Lomakin, G.B. Benedek, D.B. Teplow, *J. Mol. Biol.* **425**, 292 (2013).
- [45] W. Kim, M.H. Hecht, *J. Biol. Chem.* **280**, 35069 (2005).
- [46] E. Levy, M.D. Carman, I.J. Fernandez-Madrid, M.D. Power, I. Lieberburg, S.G. van Duinen, G.T. Bots, W. Luyendijk, B. Frangione, *Science* **248**, 1124 (1990).
- [47] K. Kamino, H.T. Orr, H. Payami et al., *Am. J. Hum. Genet.* **51**, 998 (1992).
- [48] T.J. Grabowski, H.S. Cho, J.P. Vonsattel, G.W. Rebeck, S.M. Greenberg, *Ann. Neurol.* **49**, 697 (2001).
- [49] T. Tomiyama, T. Nagata, H. Shimada et al., *Ann. Neurol.* **63**, 377 (2008).
- [50] F. Massi, J.E. Straub, *Biophys. J.* **81**, 697 (2001).
- [51] S. Côté, P. Derreumaux, N. Mousseau, *J. Chem. Theory Comput.* **7**, 2584 (2011).
- [52] Y.S. Lin, V.S. Pande, *Biophys. J.* **103**, L47 (2012).
- [53] A. Huet, P. Derreumaux, *Biophys. J.* **91**, 3829 (2006).
- [54] O. Coskuner, O. Wise-Scira, G. Perry, T. Kitahara, *ACS Chem. Neurosci.* **4**, 310 (2013).
- [55] S. Mitternacht, I. Staneva, T. Hard, A. Irback, *Proteins* **78**, 2600 (2010).
- [56] M.G. Krone, A. Baumketner, S.L. Bernstein, T. Wyttenbach, N.D. Lazo, D.B. Teplow, M.T. Bowers, J.E. Shea, *J. Mol. Biol.* **381**, 221 (2008).
- [57] A. Baumketner, M.G. Krone, J.-E. Shea, *Proc. Natl. Acad. Sci. USA* **105**, 6027 (2008).
- [58] V. Betts, M.A. Leissring, G. Dolios, R. Wang, D.J. Selkoe, D.M. Walsh, *Neurobiol. Dis.* **31**, 442 (2008).
- [59] H.A. Lashuel, D.M. Hartley, B.M. Petre, J.S. Wall, M.N. Simon, T. Walz, P.T. Lansbury Jr., *J. Mol. Biol.* **332**, 795 (2003).
- [60] L. Miravalle, T. Tokuda, R. Chiarle, G. Giaccone, O. Bugiani, F. Tagliavini, B. Frangione, J. Ghiso, *J. Biol. Chem.* **275**, 27110 (2000).
- [61] J. Davis, F. Xu, R. Deane, G. Romanov, M.L. Previti, K. Zeigler, B.V. Zlokovic, W.E. Van Nostrand, *J. Biol. Chem.* **279**, 20296 (2004).
- [62] M.R. Elkins, T. Wang, M. Nick, H. Jo, T. Lemmin, S.B. Prusiner, W.F. DeGrado, J. Stöhr, M. Hong, *J. Am. Chem. Soc.* **138**, 9840 (2016).
- [63] A.T. Petkova, W.-M. Yau, R. Tycko, *Biochem* **45**, 498 (2006).
- [64] A.K. Paravastu, R.D. Leapman, W.-M. Yau, R. Tycko, *Proc. Natl. Acad. Sci. USA* **105**, 18349 (2008).
- [65] T. Lührs, C. Ritter, M. Adrian, D. Riek-Loher, B. Bohrmann, H. Döbeli, D. Schubert, R. Riek, *Proc. Natl. Acad. Sci. USA* **102**, 17342 (2005).
- [66] T. Takeda, D.K. Klimov, *J. Phys. Chem. B* **113**, 6692 (2009).
- [67] T. Sato, P. Kienlen-Campard, M. Ahmed, W. Liu, H. Li, J.I. Elliott, S. Aimoto, S.N. Constantinescu, J.-N. Octave, S.O. Smith, *Biochem* **45**, 5503 (2006).
- [68] A.T. Petkova, Y. Ishii, J.J. Balbach, O.N. Antzutkin, R.D. Leapman, F. Delaglio, R. Tycko, *Proc. Natl. Acad. Sci. USA* **99**, 16742 (2002).
- [69] F. Massi, D. Klimov, D. Thirumalai, J.E. Straub, *Protein Sci.* **11**, 1639 (2002).
- [70] S. Verma, A. Singh, A. Mishra, *Biochim. Biophys. Acta* **1834**, 24 (2013).
- [71] Z. Lv, R. Roychaudhuri, M.M. Condrón, D.B. Teplow, Y.L. Lyubchenko, *Sci. Rep.* **3**, 2880 (2013).
- [72] H.A. Scheidt, I. Morgado, S. Rothemund, D. Huster, *J. Biol. Chem.* **287**, 2017 (2012).
- [73] B. Sarkar, V.S. Mithu, B. Chandra, A. Mandal, M. Chandrakesan, D. Bhowmik, P.K. Madhu, S. Maiti, *Angew. Chem. Int. Ed. Engl.* **53**, 6888 (2014).
- [74] B. Ma, R. Nussinov, *J. Biol. Chem.* **286**, 34244 (2011).
- [75] W. Zago, M. Buttini, T.A. Comery, C. Nishioka, S.J. Gardai, P. Seubert, D. Games, F. Bard, D. Schenk, G.G. Kinney, *Neurosci. J.* **32**, 2696 (2012).
- [76] H. Li, Z. Du, D.H. Lopes, E.A. Fradinger, C. Wang, G. Bitan, *J. Med. Chem.* **54**, 8451 (2011).
- [77] W.-T. Chen, C.-J. Hong, Y.-T. Lin, W.-H. Chang, H.-T. Huang, J.-Y. Liao, Y.-J. Chang, Y.-F. Hsieh, C.-Y. Cheng, H.-C. Liu, *PLoS One* **7**, e35807 (2012).
- [78] N.D. Lazo, M.A. Grant, M.C. Condrón, A.C. Rigby, D.B. Teplow, *Protein Sci.* **14**, 1581 (2005).
- [79] J.T. Jarrett, E.P. Berger, P.T. Lansbury Jr., *Biochem* **32**, 4693 (1993).

- [80] Y.-J. Chang, N.H. Linh, Y.H. Shih, H.-M. Yu, M.S. Li, Y.-R. Chen, *ACS Chem. Neurosci.* **7**, 1097 (2016).
- [81] N.H. Linh, T.T. Minh Thu, L. Tu, C.-K. Hu, M.S. Li, *J. Phys. Chem. B* **121**, 4341 (2017).
- [82] F. Chiti, M. Stefani, N. Taddei, G. Ramponi, C.M. Dobson, *Nature* **424**, 805 (2003).
- [83] T.T.M. Thu, N.T. Co, L.A. Tu, M.S. Li, *J. Chem. Phys.* **150**, 225101 (2019).
- [84] M.S. Li, D.K. Klimov, J.E. Straub, D. Thirumalai, *J. Chem. Phys.* **129**, 175101 (2008).
- [85] H.B. Nam, M. Kouza, H. Zung, M.S. Li, *J. Chem. Phys.* **132**, 165104 (2010).
- [86] P.I. Zhuravlev, G. Reddy, J.E. Straub, D. Thirumalai, *J. Mol. Biol.* **426**, 2653 (2014).
- [87] U. Baul, D. Chakraborty, M.L. Mugnai, J.E. Straub, D. Thirumalai, *J. Phys. Chem. B* **123**, 3462 (2019).
- [88] D. Chakraborty, J.E. Straub, D. Thirumalai, *Proc. Natl. Acad. Sci. USA* **117**, 19926 (2020).
- [89] S.W. Snyder, U.S. Ladrer, W.S. Wade, G.T. Wang, L.W. Barrett, E.D. Matayoshi, H.J. Huffaker, G.A. Krafft, T.F. Holzman, *Biophys. J.* **67**, 1216 (1994).
- [90] R. Pellarin, P. Schuetz, E. Guarnera, A. Caffisch, *J. Am. Chem. Soc.* **132**, 14960 (2010).
- [91] M. Kouza, N.T. Co, M.S. Li, S. Kmiecik, A. Kolinski, A. Kloczkowski, I.A. Buhimschi, *J. Chem. Phys.* **148**, 215106 (2018).
- [92] T.T.M. Thu, M.S. Li, *J. Chem. Phys.* **157**, 055101 (2022).
- [93] F. Franks, R.H.M. Hatley, H.L. Friedman, *Biophys. Chem.* **31**, 307 (1988).
- [94] W. Wang, C.J. Roberts, *AAPS J.* **15**, 840 (2013).
- [95] J.J. Kayser, P. Arnold, A. Steffen-Heins, K. Schwarz, J.K. Keppler, *J. Food Eng.* **270**, 109764 (2020).
- [96] R. Sabaté, M. Gallardo, J. Estelrich, *Int. J. Biol. Macromol.* **35**, 9 (2005).
- [97] Y. Kusumoto, A. Lomakin, D.B. Teplow, G.B. Benedek, *Proc. Natl. Acad. Sci. USA* **95**, 12277 (1998).
- [98] P.L. Privalov, S.J. Gill, in: *Advances in Protein Chemistry*, Vol. 39, Eds. C.B. Anfinsen, J.T. Edsall, F.M. Richards, D.S. Eisenberg, Academic Press, 1988, p. 191.
- [99] R.L. Remmele, S.D. Bhat, D.H. Phan, W.R. Gombotz, *Biochem* **38**, 5241 (1999).
- [100] P.L. Privalov, *Crit. Rev. Biochem. Mol. Biol.* **25**, 281 (1990).
- [101] B. Luan, B. Shan, C. Baiz, A. Tokmakoff, D.P. Raleigh, *Biochem* **52**, 2402 (2013).
- [102] R. Esfandiary, A. Parupudi, J. Casas-Finet, D. Gadre, H. Sathish, *J. Pharm. Sci.* **104**, 577 (2015).
- [103] A. Oliva, J.B. Fariña, M. Llabrés, *J. Chromatogr.* **1022**, 206 (2016).
- [104] M. Smith, J. Sharp, C. Roberts, *Biophys. J.* **93**, 2143 (2007).
- [105] M. Manno, E.F. Craparo, A. Podestf, D. Bulone, R. Carrotta, V. Martorana, G. Tiana, P.L. San Biagio, *J. Mol. Biol.* **366**, 258 (2007).
- [106] W. Wang, C.J. Roberts, *Int. J. Pharm.* **550**, 251 (2018).
- [107] N. Chakroun, D. Hilton, S.S. Ahmad, G.W. Platt, P.A. Dalby, *Mol. Pharm.* **13**, 307 (2016).
- [108] Z. Sahin, Y.K. Demir, V. Kayser, *Eur. J. Pharm. Sci.* **86**, 115 (2016).
- [109] A. Saluja, V. Sadineni, A. Mungikar, V. Nashine, A. Kroetsch, C. Dahlheim, V.M. Rao, *Pharm. Res.* **31**, 1575 (2014).
- [110] N.T. Co, C.K. Hu, M.S. Li, *J. Chem. Phys.* **138**, 185101 (2013).
- [111] K. Kar, M. Jayaraman, B. Sahoo, R. Kodali, R. Wetzal, *Nat. Struct. Mol. Biol.* **18**, 328 (2011).
- [112] R. Sabaté, J. Estelrich, *Biopolymers* **67**, 113 (2002).
- [113] G. Meisl, X. Yang, B. Frohm, T.P.J. Knowles, S. Linse, *Sci. Rep.* **6**, 18728 (2016).
- [114] L.O. Tjernberg, A. Pramanik, S. Björling, P. Thyberg, J. Thyberg, C. Nordstedt, K.D. Berndt, L. Terenius, R. Rigler, *Chem. Biol.* **6**, 53 (1999).
- [115] R. Sabaté, J. Estelrich, *J. Phys. Chem. B* **109**, 11027 (2005).
- [116] M. Novo, S. Freire, W. Al-Soufi, *Sci. Rep.* **8**, 1783 (2018).
- [117] T. Deva, N. Lorenzen, B.S. Vad, S.V. Petersen, I. Thürgersen, J.J. Enghild, T. Kristensen, D.E. Otzen, *Biochim. Biophys. Acta* **1834**, 677 (2013).
- [118] E.T. Powers, D.L. Powers, *Biophys. J.* **94**, 379 (2008).
- [119] K.L. Zapadka, F.J. Becher, A.L. Gomes dos Santos, S.E. Jackson, *Interface Focus* **7**, 20170030 (2017).
- [120] S. Saha, S. Deep, *Curr. Phys. Chem.* **4**, 114 (2014).
- [121] S.I.A. Cohen, S. Linse, L.M. Luheshi, E. Hellstrand, D.A. White, L. Rajah, D.E. Otzen, M. Vendruscolo, C.M. Dobson, T.P.J. Knowles, *Proc. Natl. Acad. Sci. USA* **110**, 9758 (2013).

- [122] Y.S. Kim, T.W. Randolph, M.B. Seefeldt, J.F. Carpenter, *Method Enzymol.* **413**, 237 (2006).
- [123] G.A.P. de Oliveira, M.A. Marques, M.M. Pedrote, J.L. Silva, *High Press Res.* **39**, 193 (2019).
- [124] J. Roche, J.A. Caro, D.R. Norberto, P. Barthe, C. Roumestand, J.L. Schlessman, A.E. Garcia, B.E. Garcia-Moreno, C.A. Royer, *Proc. Natl. Acad. Sci. USA* **109**, 6945 (2012).
- [125] G.A.P. de Oliveira, J.L. Silva, *Proc. Natl. Acad. Sci. USA* **112**, E2775 (2015).
- [126] S.D. Hamann, *Rev. Phys. Chem. Jpn.* **50**, 147 (1980).
- [127] R.J. St. John, J.F. Carpenter, T.W. Randolph, *Proc. Natl. Acad. Sci. USA* **96**, 13029 (1999).
- [128] D. Foguel, J.L. Silva, *Biochem* **43**, 11361 (2004).
- [129] T.W. Randolph, M. Seefeldt, J.F. Carpenter, *Biochim. Biophys. Acta.* **1595**, 224 (2002).
- [130] S. Kobayashi, Y. Tanaka, M. Kiyono, M. Chino, T. Chikuma, K. Hoshi, H. Ikeshima, *J. Mol. Struct.* **1094**, 109 (2015).
- [131] M. López de la Paz, K. Goldie, J. Zurdo, E. Lacroix, C.M. Dobson, A. Hoenger, L. Serrano, *Proc. Natl. Acad. Sci. USA* **99**, 16052 (2002).
- [132] W. Hoyer, T. Antony, D. Cherny, G. Heim, T.M. Jovin, V. Subramaniam, *J. Mol. Biol.* **322**, 383 (2002).
- [133] B. Raman, E. Chatani, M. Kihara, T. Ban, M. Sakai, K. Hasegawa, H. Naiki, C.M. Rao, Y. Goto, *Biochem* **44**, 1288 (2005).
- [134] C.C. vandenAkker, M.F.M. Engel, K.P. Velikov, M. Bonn, G.H. Koenderink, *J. Am. Chem. Soc.* **133**, 18030 (2011).
- [135] P.J. Marek, V. Patsalo, D.F. Green, D.P. Raleigh, *Biochem* **51**, 8478 (2012).
- [136] A. Abelein, J. Jarvet, A. Barth, A. Gräslund, J. Danielsson, *J. Am. Chem. Soc.* **138**, 6893 (2016).
- [137] B. Priyanka, S.K.M. Venkata, *Curr. Chem. Biol.* **14**, 216 (2020).
- [138] A.M. Tsai, J.H. van Zanten, M.J. Betenbaugh, *Biotechnol. Bioeng.* **59**, 281 (1998).
- [139] T. Arakawa, S.N. Timasheff, *Biochem* **23**, 5912 (1984).
- [140] R.A. Curtis, J. Ulrich, A. Montaser, J.M. Prausnitz, H.W. Blanch, *Biotechnol. Bioeng.* **79**, 367 (2002).
- [141] P. Gupta, S. Deep, *RSC Adv.* **5**, 95717 (2015).
- [142] M. Adachi, M. Noji, M. So, K. Sasahara, J. Kardos, H. Naiki, Y. Goto, *J. Biol. Chem.* **293**, 14775 (2018).
- [143] S. Saha, S. Deep, *J. Phys. Chem. B* **118**, 9155 (2014).
- [144] E.Y. Chi, S. Krishnan, B.S. Kendrick, B.S. Chang, J.F. Carpenter, T.W. Randolph, *Protein Sci.* **12**, 903 (2003).
- [145] A. Fatouros, T. Österberg, M. Mikaelsson, *Int. J. Pharm.* **155**, 121 (1997).
- [146] S.B. Zimmerman, S.O. Trach, *J. Mol. Biol.* **222**, 599 (1991).
- [147] M. Feig, I. Yu, P.-h. Wang, G. Nawrocki, Y. Sugita, *J. Phys. Chem. B* **121**, 8009 (2017).
- [148] R.J. Ellis, *Trends Biochem. Sci.* **26**, 597 (2001).
- [149] C. Cabaleiro-Lago, F. Quinlan-Pluck, I. Lynch, K.A. Dawson, S. Linse, *ACS Chem. Neurosci.* **1**, 279 (2010).
- [150] S. Mittal, L.R. Singh, *J. Biochem.* **156**, 273 (2014).
- [151] R.J. Ellis, A.P. Minton, *Biol. Chem.* **387**, 485 (2006).
- [152] D.A. White, A.K. Buell, T.P.J. Knowles, M.E. Welland, C.M. Dobson, *J. Am. Chem. Soc.* **132**, 5170 (2010).
- [153] A. Magno, A. Caffisch, R. Pellarin, *J. Phys. Chem. Lett.* **1**, 3027 (2010).
- [154] E.P. O'Brien, J.E. Straub, B.R. Brooks, D. Thirumalai, *J. Phys. Chem. Lett.* **2**, 1171 (2011).
- [155] Z. Zhou, J.-B. Fan, H.-L. Zhu, F. Shewmaker, X. Yan, X. Chen, J. Chen, G.-F. Xiao, L. Guo, Y. Liang, *J. Biol. Chem.* **284**, 30148 (2009).
- [156] N.T. Co, C.-K. Hu, M.S. Li, *J. Chem. Phys.* **138**, 185101 (2013).
- [157] G. Gao, M. Zhang, D. Gong, R. Chen, X. Hu, T. Sun, *Nanoscale* **9**, 4107 (2017).
- [158] D.C. Latshaw 2nd, C.K. Hall, *Biophys. J.* **109**, 124 (2015).
- [159] F. Musiani, A. Giorgetti, in: *International Review of Cell and Molecular Biology, Vol. 329, Early Stage Protein Misfolding and Amyloid Aggregation*, Ed. M. Sandal, Academic Press, 2017 p. 49.
- [160] B. Yang, D.J. Adams, M. Marlow, M. Zelzer, *Langmuir* **34**, 15109 (2018).
- [161] A. Keller, G. Grundmeier, *Appl. Surf. Sci.* **506**, 144991 (2020).
- [162] R. Vacha, S. Linse, M. Lund, *J. Am. Chem. Soc.* **136**, 11776 (2014).
- [163] D.J. Lindberg, E. Wesén, J. Björkeröth, S. Rocha, E.K. Esbjörner, *Biochim. Biophys. Acta. Biomembr.* **1859**, 1921 (2017).

- [164] A. Morriss-Andrews, F.L.H. Brown, J.-E. Shea, *J. Phys. Chem. B* **118**, 8420 (2014).
- [165] A. Rawat, R. Langen, J. Varkey, *Biochim. Biophys. Acta Biomembr.* **1860**, 1863 (2018).
- [166] M. Rabe, A. Soragni, N.P. Reynolds, D. Verdes, E. Liverani, R. Riek, S. Seeger, *ACS Chem. Neurosci.* **4**, 408 (2013).
- [167] Y.-C. Lin, C. Li, Z. Fakhraai, *Langmuir* **34**, 4665 (2018).
- [168] M. Mahmoudi, O. Akhavan, M. Ghavami, F. Rezaee, S.M.A. Ghiasi, *Nanoscale* **4**, 7322 (2012).
- [169] S.-g. Kang, T. Huynh, Z. Xia, Y. Zhang, H. Fang, G. Wei, R. Zhou, *J. Am. Chem. Soc.* **135**, 3150 (2013).
- [170] F. Zhang, H.-N. Du, Z.-X. Zhang et al., *Angew. Chem. Int. Ed.* **45**, 3611 (2006).
- [171] T. Ban, K. Morigaki, H. Yagi, T. Kawasaki, A. Kobayashi, S. Yuba, H. Naiki, Y. Goto, *J. Biol. Chem.* **281**, 33677 (2006).
- [172] R. Huang, R. Su, W. Qi, J. Zhao, Z. He, *Nat. Nanotechnol.* **22**, 245609 (2011).
- [173] K. Shezad, K. Zhang, M. Hussain, H. Dong, C. He, X. Gong, X. Xie, J. Zhu, L. Shen, *Langmuir* **32**, 8238 (2016).
- [174] N.T. Co, M.S. Li, *Biomolecules* **11**, 596 (2021).
- [175] M.Y. Aksenov, M.V. Aksenova, D.A. Butterfield, J.W. Geddes, W.R. Markesbery, *Neuroscience* **103**, 373 (2001).
- [176] X. Wang, W. Wang, L. Li, G. Perry, H.G. Lee, X. Zhu, *Biochim. Biophys. Acta.* **1842**, 1240 (2014).
- [177] M. Vaezzadeh, M. Sabbaghian, P. Yaghmaei, A. Ebrahim-Habibi, *Protein Pept. Lett.* **24**, 955 (2017).
- [178] S. Nusrat, R.H. Khan, *Prep. Biochem. Biotechnol.* **48**, 43 (2018).
- [179] A.A. Thorat, B. Munjal, T.W. Geders, R. Suryanarayanan, *J. Control Release* **323**, 591 (2020).
- [180] K. Jain, N. Salamat-Miller, K. Taylor, *Sci. Rep.* **11**, 11332 (2021).
- [181] C. Wallin, M. Friedemann, S.B. Sholts, A. Noormägi, T. Svantesson, J. Jarvet, P.M. Roos, P. Palumaa, A. Gräslund, S. Wärmländer, *Biomolecules* **10**, 44 (2019).
- [182] B. Alies, C. Hureau, P. Faller, *Metallomics* **5**, 183 (2013).
- [183] Z. Zhao, K. Engholm-Keller, M.M. Poojary, S.G. Boelt, A. Rogowska-Wrzesinska, L.H. Skibsted, M.J. Davies, M.N. Lund, *J. Agric. Food Chem.* **68**, 6701 (2020).
- [184] A. Allmendinger, Y. Ni, A. Bernhard, H. Nalenz, *PDA J. Pharm. Sci. Technol.* **76**, 52 (2022).
- [185] H. Wu, T.W. Randolph, *J. Pharm. Sci.* **109**, 1473 (2020).
- [186] K.B. Vargo, P. Stahl, B. Hwang, E. Hwang, D. Giordano, P. Randolph, C. Celentano, R. Hepler, K. Amin, *Mol. Pharm.* **18**, 148 (2021).
- [187] J. Hong, L.M. Gierasch, Z. Liu, *Biophys. J.* **109**, 144 (2015).
- [188] F. Tao, Q. Han, P. Yang, *Chem. Commun.* **59**, 14093 (2023).
- [189] A.K. Sharma, E.P. O'Brien, *Curr. Opin. Struct. Biol.* **49**, 94 (2018).
- [190] P.D. Lan, D.A. Nissley, I. Sitarik, Q.V. Van, Y. Jiang, M.S. Li, E.P. O'Brien, *J. Mol. Biol.* **436**, 168487 (2024).
- [191] K. Ezzat, M. Pernemalm, S. Pålsson et al., *Nat. Commun.* **10**, 2331 (2019).
- [192] S.A. Semerdzhiev, M.A.A. Fakhree, I. Segers-Nolten, C. Blum, M.M.A.E. Claessens, *ACS Chem. Neurosci.* **13**, 143 (2022).
- [193] T. Bhardwaj, K. Gadhave, S.K. Kapuganti et al., *Nat. Commun.* **14**, 945 (2023).
- [194] S. Nyström, P. Hammarström, *J. Am. Chem. Soc.* **144**, 8945 (2022).
- [195] J.F. Nilsson, H. Baroudi, F. Gondeaud, G. Pesce, C. Bignon, D. Ptchelkine, J. Chamieh, H. Cottet, A.V. Kajava, S. Longhi, *Int. J. Mol. Sci.* **24**, 399 (2023).
- [196] E. Michiels, K. Roose, R. Gallardo et al., *Nat. Commun.* **11**, 2832 (2020).
- [197] Ł. Mioduszewski, M. Cieplak, *Phys. Chem. Chem. Phys.* **22**, 15592 (2020).
- [198] D.Q.H. Pham, M. Chwastyk, M. Cieplak, *Front. Chem.* **10**, 1106599 (2023).
- [199] M. Cieplak, T.X. Hoang, M.O. Robbins, *Proteins* **49**, 114 (2002).
- [200] M. Cieplak, M.O. Robbins, *J. Chem. Phys.* **132**, 015101 (2010).